Journal of Zhejiang University-SCIENCE A (Applied Physics & Engineering)
ISSN 1673-565X (Print); ISSN 1862-1775 (Online)
www.jzus.zju.edu.cn; www.springerlink.com
E-mail: jzus@zju.edu.cn

Experimental approach for identifying building surface materials based on hyperspectral remote sensing imagery*

Cheng-ming YE[†1,2], Peng CUI[2], Saied PIRASTEH[3], Jonathan LI[3], Yao LI[1]

([1]*Key Laboratory of Earth Exploration and Information Technology of Ministry of Education, Chengdu University of Technology, Chengdu 610059, China*)

([2]*Institute of Mountain Hazards and Environment, Chinese Academy of Sciences, Chengdu 610041, China*)

([3]*Department of Geography and Environmental Management, Faculty of Environment, University of Waterloo, Waterloo N2L 3G1, Canada*)

[†]E-mail: rsgis@sina.com

Received Mar. 20, 2017; Revision accepted Aug. 23, 2017; Crosschecked Nov. 7, 2017

Abstract: The management of hazardous building materials poses legal and financial challenges for those in the construction, real estate, and property management fields. Building surface materials have different spectral responses in the electromagnetic energy spectrum. Remote sensors can receive the energy reflection and transmission from such materials. In this study we investigated the spectral characteristics of building materials in wavelengths ranging from 350 nm to 2500 nm. We explored a new method for identifying color steel, clay, glazed tile, and asphalt concrete using hyperspectral remote sensing based on building material spectrum characteristics. We discussed methods for extracting information about the construction materials from hyperspectral remote sensing images. We described a practical applied model, based on spectrum measurements, for the analysis of common building materials, and tested the model using hyperspectral remote sensing data from the EO-1 Hyperion sensor and Chinese airborne hyperspectral data from the pushbroom hyperspectral imager (PHI) spectrometer, covering an urban area. Our results show that building surface materials can be identified from hyperspectral remote sensing images with a reasonable quality, based on the spectral sensitivity of different building materials. For example, concrete and asphalt are more sensitive than other materials. We concluded that the proposed method based on hyperspectral remote sensing images and spectral recognition techniques is an efficient way to extract information about building materials.

Key words: Building materials; Hyperspectral remote sensing (HRS); Spectral recognition; Spectrum analysis
http://dx.doi.org/10.1631/jzus.A1700149 **CLC number:** P235

1 Introduction

Rapid access to information about the structure of building materials plays a major role in urban survey, targeting military strikes, urban planning, disaster assessment, and natural disaster compensation (Vu *et al.*, 2009; Fiumi, 2012; Kotthaus *et al.*, 2014). Spectral characteristics are one of the physical properties of building materials. In theory, the type of construction material can be determined through the study of its spectral properties. Sadezky *et al.* (2005) defined experimental conditions and analytical fitting procedures for collecting and analyzing the spectra of samples of carbonaceous materials in wavelengths 514, 633, and 780 nm. Hyperspectral remote sensing (HRS) invented in the 1980s is used to acquire more detailed spectral data by using a spectral sensor fixed on a remote flying platform. In general, multispectral remote sensing uses no more than a dozen bands, which makes it difficult to obtain material characteristics. In contrast, HRS has hundreds of bands in a wider range of the spectrum and can be used to

* Project supported by the National Key Technologies R&D Program of China (No. 2016YFB0502603) and the Key Project of Sichuan Provincial Education Department (No. 2018LG113), China
ORCID: Cheng-ming YE, http://orcid.org/0000-0002-6799-0286

capture a material's composition through its spectral response. It has a greater potential ability to identify different types of building material, but requires more complex data processing methods and experiments. Employing a hierarchical approach may enable the extraction of information about differentiated material composition, allowing mapping at the highest possible accuracy and reducing spectral confusion between materials (Franke *et al.*, 2009). Twenty years ago, HRS was not so common, and researchers used multispectral data to explore methods for classifying buildings and other things (Martin, 1993; Elnazir *et al.*, 2004; Keshava, 2004; Jin and Davis, 2005; Shahtahmassebi *et al.*, 2012). Using those applications, it was difficult to distinguish different kinds of materials. However, hyperspectral data provide more detailed information and, in theory, could even be used to diagnose damage on building surfaces. Infrared wavelengths allow the detection of moisture, salt blooming, and biological coverings, demonstrating the capabilities of multispectral techniques for the detection of damage on building surfaces. As the spectral sensitivity of different kinds of building material varies, the essence of this study relates to the microscopic structure of matter. HRS technology has become one of the hottest research topics of remote sensing applications in recent years because it can quickly obtain sunlight reflection information from buildings and spectrum information over large areas (Onojeghuo and Blackburn, 2011; Vega *et al.*, 2012). A high-level application of remote sensing classification technique provides a new approach for testing methods for extracting information from materials using remote sensing images. Spectral analysis is one of the principle techniques of HRS, and its aim is to find the spectral characteristics of absorption and reflection, such as the absorption valley and the reflection peak. Based on these spectral characteristics, HRS can be used to extract a significant quantity of information in a wide range of applications, such as agriculture, hazard management, mineral extraction, and forestry. The application of HRS is a very complex process, consisting of basic data processing, geometric correction, radiometric correction, and reflectance analysis (Tuia *et al.*, 2009; Bajorski, 2011; Fauvel *et al.*, 2013; Li *et al.*, 2015; Ran *et al.*, 2015; Geng *et al.*, 2016). Some special processes such as image filtering, water vapor removal, and spectral data compression are needed to improve the image quality.

In recent years, it has been widely agreed that spatial features derived from textural and structural imagery, and object-based methods are important information sources that complement spectral properties for the accurate classification of high-resolution urban imagery (Huang *et al.*, 2014). However, urban cover includes water, roads, buildings, and vegetation. The concept of deep learning, recently applied to hyperspectral data classification (Chen *et al.*, 2014), has shown that auto encoder (AE)-extracted features are useful for classification, and help to increase the accuracy of support vector machine (SVM) and logistic regression in agricultural cultivation regions of extensive planting. In this study, we tested and explored the relationships between spectral characteristics and building materials. The contribution of this study is to deliver a method to extract material information efficiently from urban areas.

2 Data and experimental methods

2.1 Remote sensing data and spectral data

EO-1 Hyperion images were typical hyperspectral remote sensing images and the EO-1 hyperspectral instrument provides a new class of observation data for obtaining earth surface characterizations. The Hyperion is capable of providing high resolution of surface properties using hundreds of spectral bands versus the ten multispectral bands resolved during traditional Landsat imaging missions. Through these spectral bands, complex land ecosystems can be imaged and accurately classified. The Hyperion provides detailed spectral mapping across all 220 channels with a high radiometric accuracy. The major components of the instrument include a fore-optics design system based on the Korea multi-purpose satellite (KOMPSAT) electro-optical camera (EOC) mission. The telescope provides for two separate grating image spectrometers to improve the signal-to-noise ratio (SNR). The Chinese pushbroom hyperspectral imager (PHI) is an airborne hyper-spectrometer scanning in pushing-broom with a charge-coupled device (CCD) designed to have 376 pixels per line. The sampling interval is 1.86 nm and there are up to 244 channels. It can take images at 60 frames per second, transmitting data at 7.2 Mb/s. EO-1 and PHI images covered the study area located southwest of Beijing city, China.

The spectrum data used in this study were from two sources: the Johns Hopkins University Spectral Library and measurements made by a research group in the field. The data consist of surface reflectance values and wavelengths ranging from 350 nm to 2500 nm. The 45 samples gathered from the study region were measured in the laboratory. The 12 building types covered the various kinds of materials found in the study area, such as glazed tile, color steel tile, clay tile, asphalt concrete, marble, and cement concrete. The endmember spectrum was selected from hyperspectral images, and filtered or imported from the spectrum library. Fig. 1 depicts the flowchart of the experimental methods used in this study based on HRS data and spectra extraction techniques. Some methods drew on previous studies.

2.2 Experimental methods

To identify the type of material, it is essential to extract differences in material spectral curves. In this study, spectral angle method (SAM) and spectral information divergence (SID) were used, and the results were analyzed together. The purpose of SAM (Petropoulos *et al.*, 2010; He *et al.*, 2013) in remote sensing classification algorithms is to compare one material spectrum with another that is measured in the field or collected from the spectrum library. It views every spectral as a vector space, and the distance between two vectors is determined by their similarity (Fig. 2).

The spectral curve is based on remote sensing digital number (DN) values (Mitchell and Glenn, 2009; Hadigheh and Ranjbar, 2013), and every band has a DN in-line to a vector curve. Eq. (1) calculates the degree of similarity (α) between the reference spectral $\boldsymbol{\gamma}$ and the spectral image $\boldsymbol{\tau}$ under Euclid space.

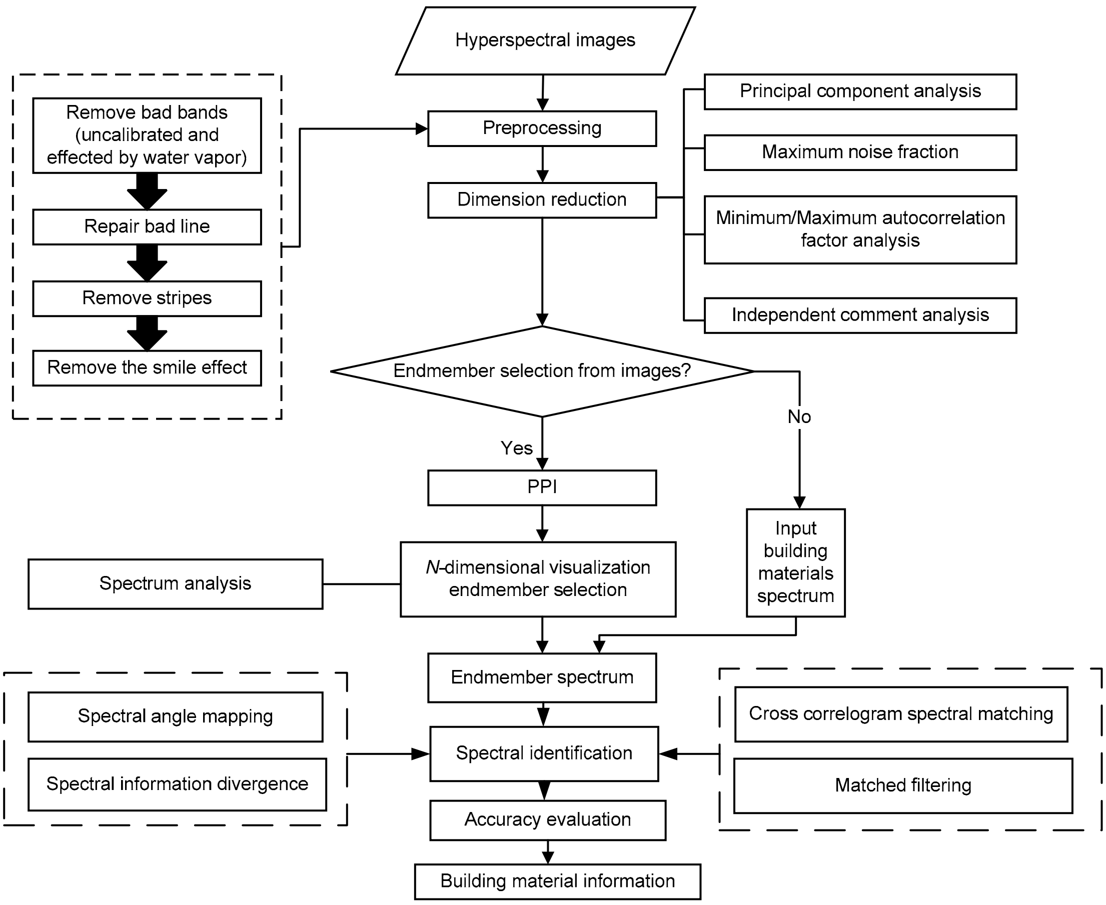

Fig. 1 Data processing flowchart (PPI represents the pixel purity index)

$$\alpha = \arccos\left(\frac{\boldsymbol{\gamma} \cdot \boldsymbol{\tau}}{\|\boldsymbol{\gamma}\| \cdot \|\boldsymbol{\tau}\|}\right). \tag{1}$$

It was supposed that two spectra vectors are $\boldsymbol{A}=(A_1, A_2, \ldots, A_N)$, $\boldsymbol{B}=(B_1, B_2, \ldots, B_N)$. A_i and B_i (i=1, 2, …, N) are vector components of $\boldsymbol{A}$ and $\boldsymbol{B}$, respectively. The spectral information divergence is SID($\boldsymbol{A}$, $\boldsymbol{B}$)=$D(\boldsymbol{A}\|\boldsymbol{B})+D(\boldsymbol{B}\|\boldsymbol{A})$ and followed by

$$\begin{cases} D(\boldsymbol{A} \| \boldsymbol{B}) = \sum_{i=1}^{N} p_i \log(p_i / q_i), \\ D(\boldsymbol{B} \| \boldsymbol{A}) = \sum_{i=1}^{N} q_i \log(q_i / p_i), \\ p_i = A_i \Big/ \sum_{i=1}^{N} A_i, \quad q_i = B_i \Big/ \sum_{i=1}^{N} B_i. \end{cases} \tag{2}$$

SID can be used to evaluate the similarity between an endmember spectral and a reference spectral by calculating their spectral information divergence (Eq. (2)). The spectral information divergence number is in the range of [0, 1], and a bigger number indicates a larger gap between two spectra.

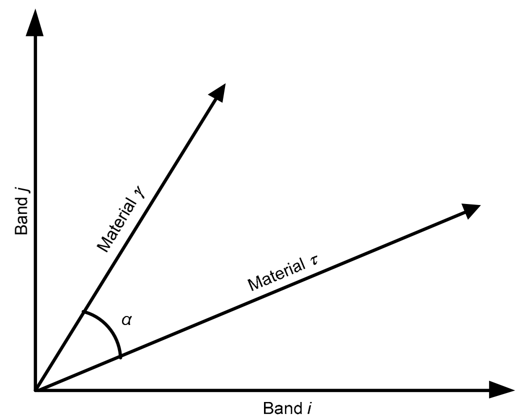

Fig. 2 Use of spectral angle method (SAM) to identify two materials

3 Results and discussion

We selected spectra from six kinds of building material (Fig. 3): glazed tile, color steel tile, clay tile, asphalt concrete, marble, and cement concrete. Fig. 4 depicts the images of building materials with a high pixel resolution. Objects could be identified as buildings using multispectral remote sensing based on imagery tone or texture. However, the challenge is to identify the type of building material. Fig. 3 shows the spectrum effect of CO_2, CO, water vapor or bad lines that is the straight line portions. The glazed tile is similar to the clay tile because they both contain clay elements. The difference is that a glazed tile is fired at high temperature and covered with glaze, whereas a clay tile is not. The wavelength range of 1150 nm to 1200 nm can be used to distinguish clay absorbed by kaolinite and SiO_2. Color steel tile had the most distinct characteristics, having a strong ability to reflect electromagnetic energy in the 1100 nm to 2500 nm range. Color steel tiles showed strong blue absorption

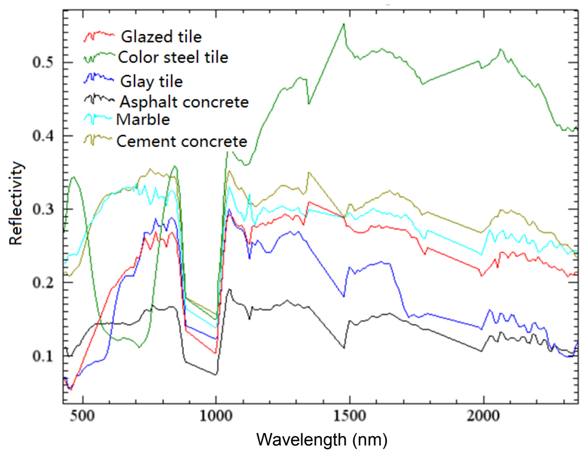

Fig. 3 Spectra from six kinds of building material (the straight linear part represents the removal bands affected by CO_2, CO, water vapor or bad lines)

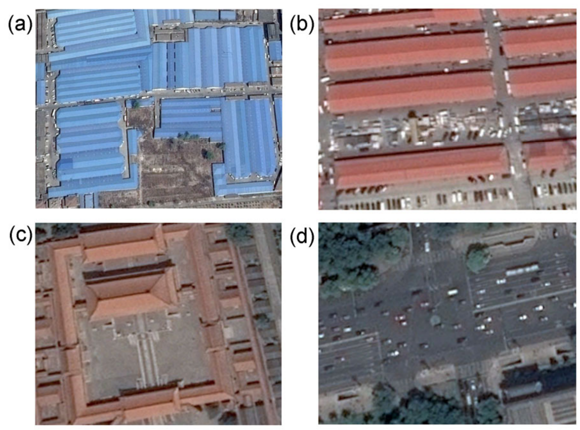

Fig. 4 High resolution images of different building materials: (a) color steel tile; (b) clay tile; (c) glazed tile; (d) asphalt concrete

in the visible light range, but a strong reflection after 1100 nm, and there was a weak absorption valley at about 1500 nm. Asphalt concrete, cement concrete, and marble had the most similar spectra because of the marble gravel element. Most differences among the materials tested were found within the distribution of the visible spectrum.

We carried out an experiment using HRS Hyperion images and Chinese airborne hyperspectral PHI data covering Beijing city, China, to extract building material information. In this experiment, the angle range was changed from 0.1 to 0.25 radians using SAM. Fig. 5 depicts the results and the identification of color steel tile and cement concrete materials extracted by the Chinese airborne hyperspectral PHI data, SAM, and SID. Figs. 5a and 5b show that SAM can provide more reliable information than SID.

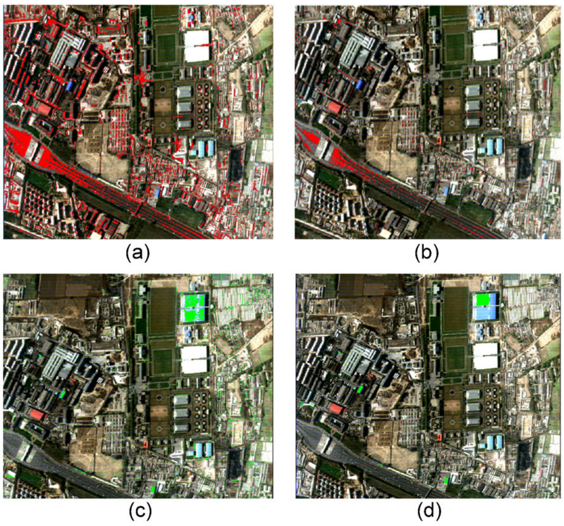

Fig. 5 Identifying materials by SAM ((a) and (c)) and SID ((b) and (d)) based on PHI imagery ((a) and (b) show cement concrete material marked red and (c) and (d) show sheet steel material marked green)

The detection accuracy of SAM was 86%, compared with 65% for SID. The cement concrete of the road near a highway toll house has been identified using SAM. Fig. 5c illustrates the color steel identified by the SAM method. In identifying the color steel of the blue building, the accuracy of SAM (91%) was much higher than that of SID (41%). The blue building is a factory with a sheet steel roof. Fig. 6 shows the distribution of six building materials based on SAM from EO-1 Hyperion imagery. The base map of Fig. 6 is the original remote sensing image based on true color band combinations.

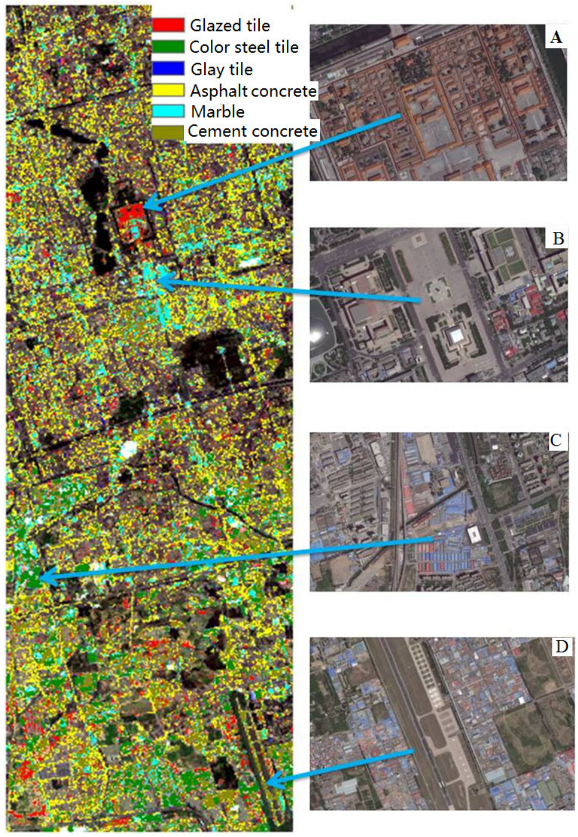

Fig. 6 Recognition results for six kinds of building material

Through spectral analysis and recognition, SAM determines building materials accurately based on their spectral sensitivity. The results show that common building materials can be identified, including color steel tile, clay tile, glazed tile, and asphalt concrete. In Fig. 6, the red color indicates clay tile, the material used in the ancient buildings of Beijing city. Most of the roof materials in the area are red glazed tile, and the Imperial Palace shows the most concentrated area of this material (area A). The green color indicates steel tile, which can be deduced as a factory roof (area C) located in the southern suburbs. We found that the optimum angle of 0.25 radians to the SAM is an appropriate parameter to recognize steel tiles. Although asphalt concrete, cement concrete, and marble spectrum curves were very similar, they could be distinguished by spectral remote sensing based on the visible light bands and near infrared.

For example, in Fig. 6, area B is Tiananmen Square in Beijing city in which all the ground is covered by marble. Area D is the Nanyuan Airport which has a cement concrete runway. The main roads in Beijing city are paved by asphalt concrete, shown in yellow. Fig. 6 shows the main transportation network framework in Beijing. These three materials were identified by the optimum angle of 0.1 radians to the SAM.

4 Conclusions

We concluded that the method based on HRS and spectral recognition techniques is an efficient way to extract building materials. However, the results of this study suggest an improved method for urban surveying that could save costs. We found that different materials have different spectral sensitivities. The angle settings are not the same when using SAM, and need to be adjusted according to the specific applications and objects. Our results show that there is a significant spectral correlation between building materials with a similar chemical composition, but they still can be distinguished based on HRS. We expect that hyperspectral data will be used more often in other applications in the future.

Acknowledgements

The authors appreciate undergraduates Zhi-ming DING and Zi-ying ZHONG (Chengdu University of Technology, China) for data processing.

References

Bajorski, P., 2011. Statistical inference in PCA for hyperspectral images. *IEEE Journal of Selected Topics in Signal Processing*, **5**(3):438-445. http://dx.doi.org/10.1109/JSTSP.2011.2105244

Chen, Y.S., Lin, Z.H., Zhao, X., *et al.*, 2014. Deep learning-based classification of hyperspectral data. *IEEE Journal of Selected Topics in Applied Earth Observations and Remote Sensing*, **7**(6):2094-2107. http://dx.doi.org/10.1109/JSTARS.2014.2329330

Elnazir, R., Feng, X.Z., Cheng, Z., 2004. Satellite remote sensing for urban growth assessment in Shaoxing City-Zhejiang Province. *Journal of Zhejiang University-SCIENCE*, **5**(9):1095-1101. http://dx.doi.org/10.1631/jzus.2004.1095

Fauvel, M., Tarabalka, Y., Benediktsson, J.A., *et al.*, 2013. Advances in spectral-spatial classification of hyperspectral images. *Proceedings of the IEEE*, **101**(3):652-675. http://dx.doi.org/10.1109/JPROC.2012.2197589

Fiumi, L., 2012. Surveying the roofs of Rome. *Journal of Cultural Heritage*, **13**(3):304-313. http://dx.doi.org/10.1016/j.culher.2011.12.003

Franke, J., Roberts, D.A., Halligan, K., *et al.*, 2009. Hierarchical multiple endmember spectral mixture analysis (MESMA) of hyperspectral imagery for urban environments. *Remote Sensing of Environment*, **113**(8):1712-1723. http://dx.doi.org/10.1016/j.rse.2009.03.018

Geng, X.R., Ji, L.Y., Sun, K., 2016. Non-negative matrix factorization based unmixing for principal component transformed hyperspectral data. *Frontiers of Information Technology & Electronic Engineering*, **17**(5):403-412. http://dx.doi.org/10.1631/FITEE.1600028

Hadigheh, S.M.H., Ranjbar, H., 2013. Lithological mapping in the eastern part of the central Iranian volcanic belt using combined ASTER and IRS data. *Journal of the Indian Society of Remote Sensing*, **41**(4):921-931. http://dx.doi.org/10.1007/s12524-013-0284-1

He, C., Zhao, Y.Y., Tian, J., *et al.*, 2013. Improving change vector analysis by cross-correlogram spectral matching for accurate detection of land-cover conversion. *International Journal of Remote Sensing*, **34**(4):1127-1145. http://dx.doi.org/10.1080/01431161.2012.718458

Huang, X., Lu, Q.K., Zhang, L.P., 2014. A multi-index learning approach for classification of high-resolution remotely sensed images over urban areas. *ISPRS Journal of Photogrammetry and Remote Sensing*, **90**:36-48. http://dx.doi.org/10.1016/j.isprsjprs.2014.01.008

Jin, X.Y., Davis, C.H., 2005. Automated building extraction from high-resolution satellite imagery in urban areas using structural, contextual, and spectral information. *EURASIP Journal on Advances in Signal Processing*, **2005**(14):2196-2206. http://dx.doi.org/10.1155/ASP.2005.2196

Keshava, N., 2004. Distance metrics and band selection in hyperspectral processing with applications to material identification and spectral libraries. *IEEE Transactions on Geoscience and Remote Sensing*, **42**(7):1552-1565. http://dx.doi.org/10.1109/TGRS.2004.830549

Kotthaus, S., Smith, T.E.L., Wooster, M.J., *et al.*, 2014. Derivation of an urban materials spectral library through emittance and reflectance spectroscopy. *ISPRS Journal of Photogrammetry and Remote Sensing*, **94**(8):194-212. http://dx.doi.org/10.1016/j.isprsjprs.2014.05.005

Li, Z.Y., Li, J., Zhou, S.L., *et al.*, 2015. Developing an algorithm for local anomaly detection based on spectral space window in hyperspectral image. *Earth Science Informatics*, **8**(4):741-749. http://dx.doi.org/10.1007/s12145-014-0200-4

Martin, J.W., 1993. Quantitative characterization of spectral ultraviolet radiation-induced photodegradation in coating systems exposed in the laboratory and the field. *Progress in Organic Coatings*, **23**(1):49-70. http://dx.doi.org/10.1016/0033-0655(93)80004-T

Mitchell, J.J., Glenn, N.F., 2009. Subpixel abundance estimates in mixture-tuned matched filtering classifications of leafy spurge (*Euphorbia esula* L.). *International Journal of Remote Sensing*, **30**(23):6099-6119. http://dx.doi.org/10.1080/01431160902810620

Onojeghuo, A.O., Blackburn, G.A., 2011. Optimising the use of hyperspectral and LiDAR data for mapping reedbed habitats. *Remote Sensing of Environment*, **115**(8):2025-2034. http://dx.doi.org/10.1016/j.rse.2011.04.004

Petropoulos, G.P., Vadrevu, K.P., Xanthopoulos, G., *et al.*, 2010. A comparison of spectral angle mapper and artificial neural network classifiers combined with landsat TM imagery analysis for obtaining burnt area mapping. *Sensors*, **10**(3):1967-1985. http://dx.doi.org/10.3390/s100301967

Ran, Q.H., Qian, Q., Li, W., *et al.*, 2015. Impact of earthquake-induced-landslides on hydrologic response of a steep mountainous catchment: a case study of the Wenchuan earthquake zone. *Journal of Zhejiang University-SCIENCE A (Applied Physics & Engineering)*, **16**(2):131-142. http://dx.doi.org/10.1631/jzus.A1400039

Sadezky, A., Muckenhuber, H., Grothe, H., *et al.*, 2005. Raman microspectroscopy of soot and related carbonaceous materials: spectral analysis and structural information. *Carbon*, **43**(8):1731-1742. http://dx.doi.org/10.1016/j.carbon.2005.02.018

Shahtahmassebi, A., Yu, Z.L., Wang, K., *et al.*, 2012. Monitoring rapid urban expansion using a multi-temporal RGB-impervious surface model. *Journal of Zhejiang University-SCIENCE A (Applied Physics & Engineering)*, **13**(2):146-158. http://dx.doi.org/10.1631/jzus.A1100034

Tuia, D., Ratle, F., Pacifici, F., *et al.*, 2009. Active learning methods for remote sensing image classification. *IEEE Transactions on Geoscience and Remote Sensing*, **47**(7): 2218-2232. http://dx.doi.org/10.1109/TGRS.2008.2010404

Vega, S.H., Huaman, D.L., Manian, V., 2012. Object segmentation in hyperspectral images using active contours and graph cuts. *International Journal of Remote Sensing*, **33**(4):1246-1263. http://dx.doi.org/10.1080/01431161.2011.560208

Vu, T.T., Yamazaki, F., Matsuoka, M., 2009. Multi-scale solution for building extraction from LiDAR and image data. *International Journal of Applied Earth Observation and Geoinformation*, **11**(4):281-289. http://dx.doi.org/10.1016/j.jag.2009.03.005

中文概要

题　目：基于高光谱遥感影像的建筑物表面材质识别方法

目　的：建筑物的材质信息是灾害评估和城市调查等领域的重要信息。本文旨在利用高光谱遥感影像提取地面建筑物的表面材质信息（包括材质类型和主要组成成份），并对提取方法进行对比，给出应用建议。

创新点：对建筑物材料进行光谱测试，并对其高光谱响应规律进行分析，找出有诊断意义的光谱位置；基于实验和验证得出应用方法的适应性，以提高信息提取精度。

方　法：1. 设计建筑物材质信息提取流程（图 1），并对高光谱数据进行基础处理；2. 对建筑物材料进行光谱测试（波长范围为 350~2500 nm，图 3），并完成各类建筑物的诊断性光谱分析；3. 利用光谱角度法（公式（1））和光谱信息散度法（公式（2））进行材质信息提取（图 5 和 6）；4. 综合分析两种方法的应用过程与控制参数和准确率的关系。

结　论：1. 两种方法皆可提取建筑物材质信息，但在应用过程中需要进行参数的适应性调整，这是提高准确率的关键；2. 在建筑物材质信息提取方面，光谱角度法的提取准确率略高于光谱散度法。

关键词：建筑物材料；高光谱遥感；光谱分析；光谱识别